energies

MDPI

Article

Research on Source–Grid–Load–Storage Coordinated Optimization and Evolutionarily Stable Strategies for High Renewable Energy

Yu Shi [1], Yiwen Yao [1], Yiran Li [2], Jing Wang [1], Rui Zhou [3], Xiaomin Lu [1], Xinhong Wang [1], Dingheng Wang [1], Xuefeng Gao [1], Xin Xu [1], Zilai Ou [2], Leilei Jiang [2] and Zhe Ma [2,*]

[1] Power Economic Research Institute of Jilin Electric Power Co., Ltd., Changchun 130021, China
[2] State Key Laboratory of Coastal and Offshore Engineering, Dalian University of Technology, Dalian 116024, China
[3] State Grid Jilin Electric Power Co., Ltd., Changchun 130021, China
* Correspondence: deep_mzh@dlut.edu.cn

Abstract

In the context of large-scale renewable energy integration driven by China's dual-carbon goals, and under distribution network scenarios with continuously increasing shares of wind and photovoltaic generation, this paper proposes a source–grid–load–storage coordinated planning method embedded with a multi-agent game mechanism. First, the interest transmission pathways among distributed generation operators (DGOs), distribution network operators (DNOs), energy storage operators (ESOs), and electricity users are mapped, based on which a profit model is established for each stakeholder. Building on this, a coordinated planning framework for active distribution networks (DN) is developed under the assumption of bounded rationality. Through an evolutionary-game process among DGOs, DNOs, and ESOs, and in combination with user-side demand response, the model jointly determines the optimal network reinforcement scheme as well as the optimal allocation of distributed generation (DG) and energy storage system (ESS) resources. Case studies are then conducted to verify the feasibility and effectiveness of the proposed method. The results demonstrate that the approach enables coordinated planning of DN, DG, and ESS, effectively guides users to participate in demand response, and improves both planning economy and renewable energy accommodation. Moreover, by explicitly capturing the trade-offs among multiple stakeholders through evolutionary-game interactions, the planning outcomes align better with real-world operational characteristics.

Keywords: source–grid–load–storage; multi-agent coordination; evolutionary game; demand response

Check for updates

Received: 16 December 2025
Revised: 9 January 2026
Accepted: 12 January 2026
Published: 14 January 2026

Copyright: © 2026 by the authors. Licensee MDPI, Basel, Switzerland. This article is an open access article distributed under the terms and conditions of the Creative Commons Attribution (CC BY) license.

1. Introduction

Under the accelerated implementation of China's dual-carbon strategy, the installed capacity of renewable energy sources such as wind and photovoltaic power in distribution networks (DNs) continues to grow. Their high-penetration integration introduces pronounced variability, intermittency, and uncertainty into the system [1,2]. The rapid fluctuations and spatially uneven distribution of renewable energy output can easily trigger issues such as voltage violations, reverse power flows, line overloading, and renewable curtailment, thereby posing severe challenges to the traditional "passive accommodation"

operating paradigm of conventional DNs [3–5]. To enhance renewable energy accommodation and improve system flexibility, a coordinated source–grid–load–storage (SGLS) optimization framework is established by integrating multiple flexible resources—including distributed generation (DG), energy storage systems (ESSs), flexible loads, and demand response (DR). This enables the DN to transition from a "passive response" mode toward an "active control" paradigm [6–10].

However, flexibility resources are typically invested in and operated by different stakeholders, resulting in pronounced differences in their objectives and behavioral incentives: distributed generation operators (DGOs) seek to maximize generation revenues; distribution network operators prioritize network reinforcement costs and operational security; energy storage operators (ESOs) rely on price arbitrage for profit; and users aim to reduce energy expenditures through DR. The coupling of objectives and the inherent conflicts of interest among these agents impart strong game-theoretic characteristics to DN planning. Without an effective coordination mechanism, planning decisions are prone to becoming suboptimal or even mutually constraining [11].

In recent years, extensive research has been conducted on scenarios with high renewable energy penetration. Some studies focus on enhancing the flexibility of active DNs, for example, by integrating energy storage, exploiting multi-energy complementarity, or leveraging integrated energy systems to improve the accommodation capability of renewable resources [12,13]. Mao et al. [14] unified flexible resources such as electric vehicles, hydrogen storage, and HVAC loads as "generalized energy storage" and coordinated them across day-ahead, intra-day, and real-time timescales to address renewable uncertainty, thereby improving system cost-effectiveness and reliability. Liu et al. [15] propose a source–grid expansion planning framework for incremental DN that coordinates DG deployment, line construction, and network investments to enhance power quality and renewable energy accommodation. Another body of research focuses on the coordinated planning of transmission–DNs or wind-PV–storage systems, where second-order cone relaxation and decomposition-based coordination algorithms are employed to improve the computational efficiency of large-scale planning models [6]. Saldaña-González et al. [16] apply Long Short-Term Memory-based forecasting for load and DG, coupling time-series prediction with the planning model to improve the accuracy of long-term DN expansion decisions. Li et al. [11] incorporate distribution locational marginal pricing and distributed market mechanisms into DN planning to strengthen the alignment between planning schemes and the evolving electricity market environment. Mehrjerdi [17] develop an energy storage planning model that simultaneously achieves peak shaving and voltage support, leveraging the reactive power regulation capability of inverters to improve power quality and enhance storage investment returns. Gao et al. [7] introduce a Kullback–Leibler divergence-based distributionally robust planning method that integrates multiple forms of DR—including interruptible loads (IL) and transferable loads (TL)—and coordinates with multi-energy stations to increase DN flexibility. Suryakiran et al. [18] formulate a DSO-based day-ahead market coordination model that improves active DN operational efficiency through flexible resource scheduling and price-driven signals. Mao et al. [19] provide a state-of-the-art review on the optimal operation of CCHP systems under high-penetration renewables, summarizing flexibility-enabled and uncertainty-aware scheduling (robust/stochastic/hybrid and data-driven methods) and identifying open issues in multi-energy coupling, computational tractability, and multi-stakeholder coordination across timescales—insights that motivate our SGLS coordinated planning model for active distribution networks.

Meanwhile, the trend toward market-oriented multi-agent interaction has become increasingly prominent, prompting researchers to incorporate methods such as Stackelberg games, multi-level games, and system dynamics to characterize strategic competition and interest trade-offs among participants [20,21]. Zhou et al. [22] develop an evolutionary-game model among generation entities to analyze the profit evolution of virtual power plants under different strategic choices, providing theoretical support for market operations involving multiple stakeholders. Wu et al. [23] propose a bi-level robust game-theoretic planning framework for DNs and microgrids, aiming to account for bilateral energy transactions among diverse stakeholders in emerging electricity markets. The framework employs a linear robust dual formulation to address non-convexities induced by renewable energy uncertainty. Singh et al. [24] introduce a three-layer hierarchical decision-making approach for multi-microgrid energy management in active distribution systems, which coordinates energy resources across various operational agents—including distribution companies, microgrid operators, and end users. Li et al. [25] present a two-stage dynamic robust DN planning method that accounts for correlation structures, addressing reliability challenges arising from the widespread presence of heterogeneous load entities.

Although existing studies have made significant progress in areas such as flexibility enhancement in active DN, coordinated transmission–distribution planning, multi-agent game mechanisms, and data-driven scenario generation, several limitations remain. First, the interests and behavioral patterns of multiple stakeholders are often simplified as static or one-shot decisions, which fails to capture the strategy evolution of SGLS participants under long-term and dynamic interactions. Second, few studies integrate DG, energy storage, DN operation, and DR within a unified evolutionary-game framework, making it difficult to systematically analyze how multi-agent competition–cooperation relationships influence DN planning and renewable energy accommodation. Therefore, constructing an evolutionary-game-based coordinated planning model that characterizes bounded rationality, multi-round decision-making, and adaptive strategy adjustment is of both theoretical significance and practical value for supporting high renewable penetration in active DN involving multiple stakeholders.

Motivated by these gaps, this paper proposes an evolutionary-game-driven SGLS coordinated planning approach for active DN. By modeling the strategy adaptation processes of DGOs, DNOs, ESOs, and users under price signals, revenue mechanisms, and risk constraints, the proposed method enables planning decisions driven by multi-agent behavioral evolution. This framework provides a new pathway for enhancing renewable energy accommodation, reducing DN reinforcement costs, and improving system flexibility.

2. Stakeholder Game Relationships

In a market-oriented power system, the divergent objectives and revenue preferences of different participants inevitably give rise to conflicts of interest, thereby forming a landscape of mutual constraints and strategic interactions. Achieving benefit alignment among multiple agents in complex DN planning—and motivating all parties to jointly participate in network development and improve overall planning performance—first requires a clear understanding of the benefit flows and information exchange pathways among DGOs, DNOs, ESOs, and electricity users. Accordingly, this study analyzes the interrelations and interactions among these stakeholders, as illustrated in Figure 1.

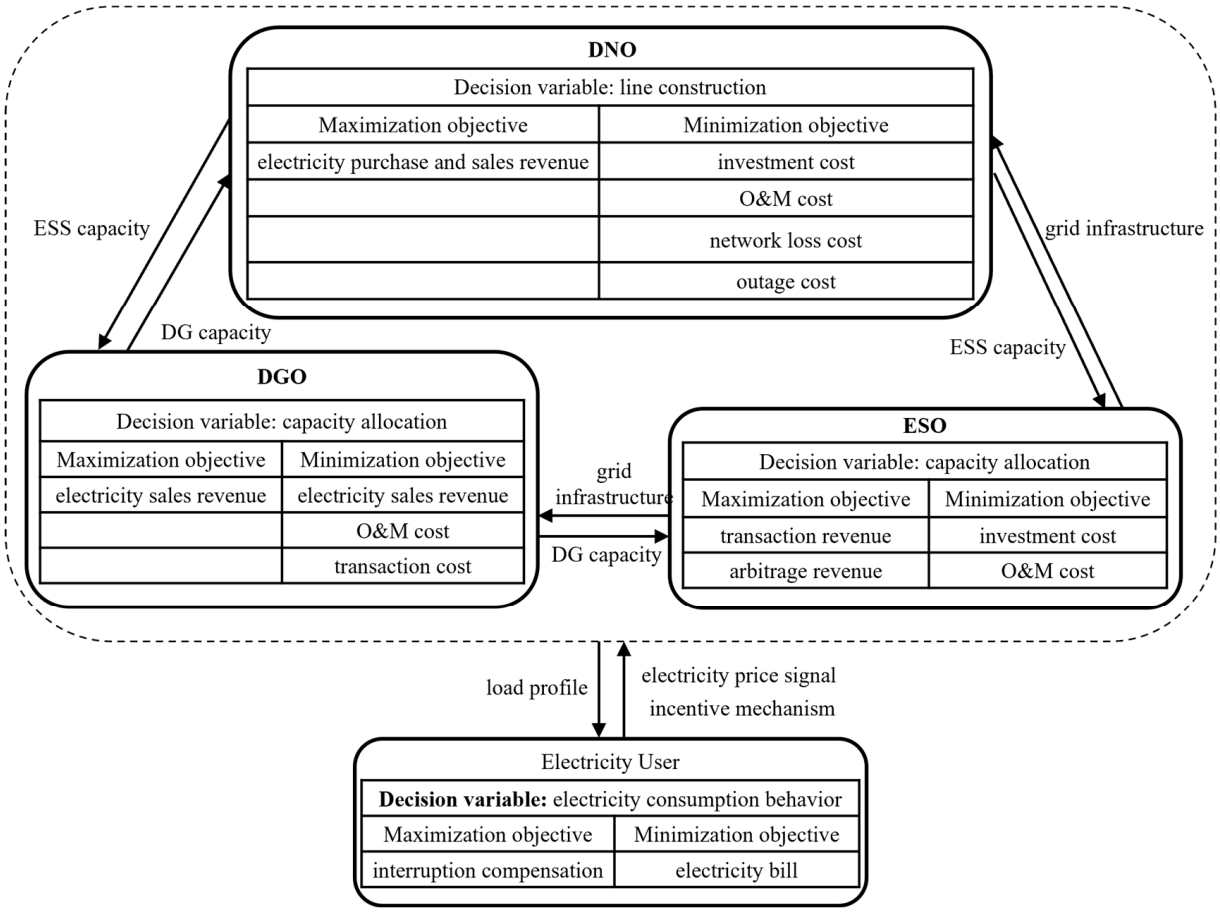


Figure 1. Interaction and information flow among stakeholders.

In SGLS coordinated planning, each participant exhibits distinct priorities. The storage business model adopted in this work assumes that ESSs purchase electricity preferentially from DG units, with additional electricity procured from the DN when necessary. To reduce renewable curtailment, ESOs first engage in bilateral transactions with DGOs and leverage the remaining battery capacity to perform price arbitrage—charging during low-price periods and discharging during high-price periods under the time-of-use (TOU) tariff. DGOs determine their capacity investments by considering construction and operation and maintenance (O&M) costs, expected electricity sales revenue, and potential income from green certificate trading.

DG capacity not only affects the traded electricity volume and revenue between ESOs and DGOs but also influences the power purchase and sales costs of DNOs. DNOs aim to ensure secure and economic grid operation, striving to minimize network reinforcement and operational costs while maintaining supply reliability. Their grid expansion decisions, however, constrain the maximum allowable DG hosting capacity, which in turn affects the profitability of ESOs. When determining ESS capacity, ESOs weigh DG–ESS transaction profits, arbitrage revenues from "low-price charging and high-price discharging," and ESS investment and operating costs. The resulting storage scale then feeds back to DG curtailment levels and affects the DNOs' grid reinforcement requirements and operational expenditures.

These interactions demonstrate that DGOs, DNOs, and ESOs have partially aligned yet interdependent interests. By contrast, electricity users participating in DR primarily focus on reducing electricity bills and improving compensation under outage or incentive mechanisms. As user benefits are largely determined by electricity prices and incentive schemes—and are not directly affected by the decision variables of the three main market

players—this study does not include users as game participants. Instead, users are modeled as external actors that adjust their consumption in response to predefined tariffs and incentives to maximize their own benefits, with their DR outcomes unidirectionally fed back to the DNOs.

3. Profit Models of Stakeholders

3.1. Profit Model of DGOs

(1) Objective function

This study considers the coordinated planning of wind and photovoltaic generation to achieve wind–solar complementarity. DGOs aim to reduce construction and operation costs and maximize revenues from electricity sales to the DN and ESSs, as well as income from green certificate trading. Accordingly, DGOs determine the installed capacity of DG based on the objective of maximizing its own profit. The objective function is defined as

$$\max F_{\mathrm{dg}} = F_{\mathrm{dg,sel}} + F_{\mathrm{ess,sel}} - C_{\mathrm{dg,con}} - C_{\mathrm{dg,ope}} \tag{1}$$

$$F_{\mathrm{dg,sel}} = \sum_{t=1}^{T}\left(\sum_{w=1}^{W} E_{\mathrm{dg,WT}} P_{\mathrm{WT},w}^{t} + \sum_{v=1}^{V} E_{\mathrm{dg,PV}} P_{\mathrm{PV},v}^{t}\right) \tag{2}$$

$$F_{\mathrm{ess,sel}} = \sum_{t=1}^{T} E_{\mathrm{dg,ess}} P_{\mathrm{chl}}^{t} \tag{3}$$

$$C_{\mathrm{dg,con}} = \sum_{w=1}^{W} \frac{N_{\mathrm{WT},w} \mathrm{P}_{\mathrm{dg}}^{\mathrm{WT},w} E_{\mathrm{dg,con}}^{\mathrm{WT},w} r(1+r)^{T_{\mathrm{dg}}^{\mathrm{WT},w}}}{(1+r)^{T_{\mathrm{dg}}^{\mathrm{WT},w}} - 1} + \sum_{v=1}^{V} \frac{\mathrm{N}_{\mathrm{PV},v} P_{\mathrm{dg}}^{\mathrm{PV},v} \mathrm{E}_{\mathrm{dg,con}}^{\mathrm{PV},v} r(1+r)^{T_{\mathrm{dg}}^{\mathrm{PV},v}}}{(1+r)^{T_{\mathrm{dg}}^{\mathrm{PV},v}} - 1} \tag{4}$$

$$C_{\mathrm{dg,ope}} = \sum_{t=1}^{T}\sum_{w=1}^{W} E_{\mathrm{dg,ope}}^{\mathrm{WT},w} P_{\mathrm{WT},w}^{t,\mathrm{pro}} + \sum_{t=1}^{T}\sum_{v=1}^{V} E_{dg,ope}^{PV,v} P_{PV,v}^{t,pro} \tag{5}$$

where F_{dg} denotes the annual net revenue of DGOs; $F_{\mathrm{dg,sel}}$ represents the electricity sales revenue obtained by DGOs; $F_{\mathrm{ess,sel}}$ denotes the revenue earned from selling electricity to ESOs; $C_{\mathrm{dg,con}}$ is the investment cost of DG construction, expressed in annualized form using the capital recovery factor to account for equipment lifetime. The annualized cost of lines and energy storage systems is treated in the same manner. For equipment lifetime n, the capital recovery factor is given by $r(1+r)^n/[(1+r)^n - 1]$ where r is the discount rate. $C_{\mathrm{dg,ope}}$ represents the O&M cost of the DG units.; T denotes the number of operating periods; w denotes the number of wind turbine (WT) types, and v denotes the number of photovoltaic (PV) types; $P_{\mathrm{WT},w}^{\mathrm{t}}$ is the actual output of WT type w in period t, and; $P_{\mathrm{PV},\nu}^{\mathrm{t}}$ denotes the actual output of PV type v in period t; $E_{\mathrm{dg,WT}}$ and $E_{\mathrm{dg,PV}}$ are the unit electricity sale prices for WT and PV generation, respectively; $E_{\mathrm{dg,ess}}$ denotes the transaction electricity price between DGOs and ESOs; P_{ch1}^{t} represents the charging power traded between the ESO and the DGO during time period t. $N_{\mathrm{WT,w}}$ represents the number of installed WTs of type w; $P_{\mathrm{dg}}^{\mathrm{WT,w}}$ is the rated power of a single WT of type w; $E_{\mathrm{dg,con}}^{\mathrm{WT,w}}$ denotes the unit capacity investment cost of WT type w. $N_{\mathrm{PV},\nu}$ is the number of PV units of type v; $P_{\mathrm{dg}}^{\mathrm{PV},\nu}$ is the rated capacity of a single PV unit of type v; $E_{\mathrm{dg,con}}^{\mathrm{PV},\nu}$ denotes the unit capacity investment cost of PV type v; $T_{\mathrm{dg}}^{\mathrm{WT},\nu}$ and $T_{\mathrm{dg}}^{\mathrm{PV},\nu}$ are the lifetimes of WT type w and PV type v, respectively; $\mathrm{E}_{\mathrm{dg,ope}}^{\mathrm{WT},\nu}$ denotes the O&M cost per unit energy output of WT type w, and; $P_{\mathrm{WT},w}^{t,\mathrm{pro}}$ is its scheduled output in period t; $E_{\mathrm{dg,ope}}^{\mathrm{PV},\nu}$ represents the O&M cost of a single PV unit of type v; $P_{\mathrm{PV},v}^{t,\mathrm{pro}}$ denotes the scheduled PV output in period t.

(2) Constraints

DG installation quantity constraints

$$N_{WT} \leq N_{WT,max} \tag{6}$$

$$N_{PV} \leq N_{PV,max} \tag{7}$$

where $N_{\mathrm{WT,max}}$ denotes the upper limit on the number of installed WTs, and $N_{\mathrm{PV,max}}$ represents the maximum allowable number of installed PV units.

Output constraints of DG units:

$$0 \leq P_{dg,WT}^{t} \leq P_{dg,WT}^{t,pro} \tag{8}$$

$$0 \leq P_{dg,PV}^{t} \leq P_{dg,PV}^{t,pro} \tag{9}$$

3.2. Profit Model of DNOs

(1) Objective function

DNOs seek to ensure secure and economic operation of the DN by jointly considering electricity purchase and sales revenues, network reinforcement costs, network loss costs, and fault-related costs. Accordingly, DNOs determine the network expansion plan with the objective of maximizing its net profit. The objective function is formulated as

$$\max F_{\mathrm{dn}} = F_{\mathrm{dn,sel}} - C_{\mathrm{dn,ch}} - C_{\mathrm{dn,line}} - C_{\mathrm{dn,loss}} - C_{\mathrm{dn,fau}} - C_{\mathrm{dn,aba}} \tag{10}$$

$$W_{\mathrm{dn,sel}} = \sum_{t=1}^{T} E_{\mathrm{dn,sel}}^{t} P_{\mathrm{dn}}^{t} \tag{11}$$

$$\mathrm{C_{dn,ch}} = \mathrm{C_{dn,grid}} + \mathrm{C_{dn,up}} \tag{12}$$

$$\mathrm{C_{dn,line}} = \frac{\mathrm{r}(1+r)^{\mathrm{T_L}}}{(1+r)^{\mathrm{T_L}} - 1} \sum_{\mathrm{l}=1}^{N_{\mathrm{l}}} C_{\mathrm{l}} L_{\mathrm{l}} \tag{13}$$

$$\mathrm{C_{dn,loss}} = \sum_{\mathrm{t}=1}^{\mathrm{T}} P_{\mathrm{dn,loss}}^{\mathrm{t}} \mathrm{E_{dn,sel}^{t}} \tag{14}$$

$$\mathrm{C_{dn,fau}} = \sum_{\mathrm{t}=1}^{\mathrm{T}} P_{\mathrm{ENS}}^{\mathrm{t}} \mathrm{E_{dn,sel}^{t}} \tag{15}$$

$$\mathrm{C_{dn,aba}} = \sum_{\mathrm{t}=1}^{\mathrm{T}} (P_{\mathrm{dn,aba}}^{\mathrm{t,WT}} \mathrm{E_{dn,aba}^{WT}} + P_{\mathrm{dn,aba}}^{\mathrm{t},PV} \mathrm{E_{dn,aba}^{PV}}) \tag{16}$$

where F_{dn} denotes the annual net revenue of the DNO; $F_{\mathrm{dn,sel}}$ represents the electricity sales revenue of the DNO; $C_{\mathrm{dn,ch}}$ is the electricity purchase cost; $C_{\mathrm{dn,line}}$ denotes the network reinforcement (line investment) cost; $C_{\mathrm{dn,loss}}$ is the cost associated with network losses; $C_{\mathrm{dn,fau}}$ denotes the cost of supply interruptions or failures; $C_{\mathrm{dn,aba}}$ represents the cost incurred due to WT and PV curtailment; $E_{\mathrm{dn,sel}}^{t}$ is the unit electricity selling price in period t; $P_{\mathrm{g}}^{\mathrm{t}}$ denotes the electricity sales volume in period t; $C_{\mathrm{dn,grid}}$ represents the cost of electricity purchased from the local grid, and $C_{\mathrm{dn,up}}$ denotes the cost of electricity purchased from the upper-level grid; T_{L} is the lifetime of distribution lines; $C_{\mathrm{dn,line}}$ denotes the investment cost for newly constructed lines; N_{l} is the total number of new lines; C_{l} represents the unit-length construction cost of the new lines; L_{l} is the length of the l-th new line; $P_{\mathrm{dn,loss}}^{t}$ denotes the network loss in period t; $P_{\mathrm{ENS}}^{\mathrm{t}}$ represents the expected energy-not-served in period t; $E_{\mathrm{dn,aba}}^{\mathrm{WT}}$ and $E_{\mathrm{dn,aba}}^{PV}$ denote the unit penalty cost for curtailed WT power and curtailed PV

power, respectively; $P_{\mathrm{dn,aba}}^{\mathrm{t,WT}}$ is the amount of WT power curtailment in period t; $P_{\mathrm{dn,aba}}^{\mathrm{t,PV}}$ is the amount of PV power curtailment in period t.

(2) Constraints

Branch power flow constraints:

$$\begin{cases} P_{Si} - P_{Li} = U_i \sum\limits_{j \in i} U_j \left(G_{ij}\, cos\theta_{ij} + B_{ij}\, sin\theta_{ij} \right) \\ Q_{Si} - Q_{Li} = U_i \sum\limits_{j \in i} U_j \left(G_{ij}\, sin\theta_{ij} - B_{ij}\, sin\theta_{ij} \right) \end{cases} \tag{17}$$

where P_{Si} denotes the total active power injected at node i by the DG units and ESSs; Q_{Si} represents the total reactive power injected at node i; P_{Li} is the sum of the active power consumed by the loads connected to node i and the charging power absorbed by the energy storage systems; Q_{Li} denotes the total reactive power consumed by the loads at node i; U_i and U_j are the voltage magnitudes at nodes i and j, respectively; G_{ij} and B_{ij} represent the conductance and susceptance of the line between nodes i and j; θ_{ij} is the voltage phase-angle difference between nodes i and j.

Nodal voltage constraints:

$$U_{i,min} \le U_i \le U_{i,max} \tag{18}$$

where $U_{i,min}$ and $U_{i,max}$ denote the lower and upper bounds of the voltage magnitude at node i, respectively.

Line power flow constraints:

$$P_{ij} \le P_{ij,max} \tag{19}$$

where P_{ij} denotes the active power transmitted through the line between nodes i and j, and $P_{ij,\max}$ represents the maximum allowable active power flow on that line.

3.3. Profit Model of ESOs

(1) Objective function

ESOs aim to maximize their total profit by increasing revenue from electricity transactions with DGOs and from price-arbitrage activities—charging during low-price periods and discharging during high-price periods—while minimizing the construction and operation costs of the ESS. Accordingly, ESOs determine the installed storage capacity based on the objective of profit maximization. The objective function is formulated as

$$\max F_{\mathrm{ess}} = F_{\mathrm{ess,ptv}} + F_{\mathrm{ess,sub}} - C_{\mathrm{ess,bus}} - C_{\mathrm{ess,con}} - C_{\mathrm{ess,ope}} \tag{20}$$

$$C_{\mathrm{ess,bus}} = F_{\mathrm{ess,sel}} \tag{21}$$

$$F_{\mathrm{ess,ptv}} = \sum_{t=1}^{T} E_{\mathrm{dn,sel}}^{t} \left(P_{\mathrm{dch2}}^{t} - P_{\mathrm{ch2}}^{t} \right) \tag{22}$$

$$F_{\mathrm{ess,sub}} = \sum_{t=1}^{T} E_{\mathrm{ess,sub}}\, P_{\mathrm{ch1}}^{t} \tag{23}$$

$$C_{\mathrm{ess,con}} = \frac{E_{\mathrm{ess,con}} N_{\mathrm{ess}} P_{\mathrm{ess}} r (1+r)^{T_{\mathrm{ess}}}}{(1+r)^{T_{ess}} - 1} \tag{24}$$

$$C_{\mathrm{ess,ope}} = E_{\mathrm{s,ope}} N_s \tag{25}$$

where F_{ess} denotes the annual net revenue of ESOs; $F_{\mathrm{ess,ptv}}$ represents the revenue earned from price arbitrage (charging at low prices and discharging at high prices); $F_{\mathrm{ess,sub}}$ denotes the government subsidies received by ESOs; $C_{\mathrm{ess,con}}$ is the construction cost of the ESS;

$C_{\text{ess,bus}}$ represents the electricity purchase cost from DGOs; $C_{\text{ess,ope}}$ denotes the O&M cost of the ESS; P^t_{dch2} and P^t_{ch2} represent the discharging and charging power of the storage system in period t, respectively, associated with price arbitrage activities; $E_{\text{ess,sub}}$ is the subsidy amount provided by the government; $E_{\text{ess,con}}$ denotes the unit capacity construction cost of the ESS; P_{s} is the rated capacity of a single storage unit; N_{s} represents the number of installed storage units; T_{ess} is the service lifetime of the storage system; $E_{\text{ess,ope}}$ denotes the O&M cost per kilowatt-hour of storage capacity.

The charging and discharging power of the ESS are expressed in Equations (26) and (27):

$$P^t_{\text{dch}} = (P^{t-1}_{\text{ess,sur}} - P^t_{\text{ess,sur}})\eta_{\text{dch}} \tag{26}$$

$$P^t_{\text{ch}} = (P^t_{\text{ess,sur}} - P^{t-1}_{\text{ess,sur}})/\eta_{\text{ch}} \tag{27}$$

where $P^{t-1}_{\text{s,sur}}$ and $P^t_{\text{s,sur}}$ denote the state of charge (SOC) of the ESS at the end of periods $t-1$ and t, respectively; η_{dch} is the discharging efficiency of the storage system; η_{ch} represents the charging efficiency. The SOC of the ESS in period t is given by

$$S^t_{ess} = \frac{P^t_{ess,sur}}{P_{ess}} \tag{28}$$

(2) Constraints

Energy storage installation quantity constraint:

$$N_{\text{ess}} \leq N_{\text{ess,max}} \tag{29}$$

where $N_{\text{ess,max}}$ denotes the upper limit on the number of installed energy storage units.

SOC constraints of the ESS:

$$S_{\text{ess,min}} \leq S^t_{ess} \leq S_{\text{ess,max}} \tag{30}$$

where $S_{\text{ess,max}}$ and $S_{\text{ess,min}}$ denote the upper and lower bounds of the SOC of the ESS, respectively.

Charging and discharging power constraints of the ESS:

$$0 \leq P^t_{ch1} + P^t_{ch2} \leq P_{ch,max} \tag{31}$$

$$0 \leq P^t_{dch1} + P^t_{dch2} \leq P_{dch,max} \tag{32}$$

where $P_{\text{ch,max}}$ and $P_{\text{dch,max}}$ denote the rated charging and discharging power of the ESS, respectively; P^t_{dch1} represents the discharging power traded between ESOs and DGOs in period t.

Charging and discharging power constraints for transactions between ESOs and DGOs:

$$\eta_{\text{ch}} \sum_{t=1}^{T} P^t_{ch1} = \sum_{t=1}^{T} \frac{P^t_{dch1}}{\eta_{dch}} \tag{33}$$

$$0 \leq P^t_{ch1} \leq P^t_{dg,pro} - P^t_{dg} \tag{34}$$

Charging and discharging state constraints of the ESS:

$$x^t_{\text{ch}} + x^t_{\text{dch}} \leq 1 \tag{35}$$

where x^t_{ch} and x^t_{dch} denote the charging and discharging state variables of the ESS in period t, respectively, and $x^t_{\text{ch}} \in [0,1]$, where $x^t_{\text{ch}} = 0$ indicates that the ESS is not charging in

period t, and $x^t_{\mathrm{ch}} = 1$ indicates that it is in the charging state. Similarly, $x^t_{\mathrm{dch}} \in [0, 1]$, where $x^t_{\mathrm{dch}} = 0$ indicates that the ESS is not discharging in period t, and $x^t_{\mathrm{dch}} = 1$ indicates that it is in the discharging state t. Equation (35) ensures that the ESS cannot be in the charging and discharging states simultaneously.

3.4. Profit Model of Electricity Users

Electricity users determine their DR actions based on electricity price signals and incentive mechanisms provided by the DNO, with the objective of maximizing their satisfaction—or equivalently, their net benefit—from participating in load response programs. Two types of DR are considered in this study: IL and TL. IL refers to the reduction in electricity consumption during peak periods without altering consumption in other periods, in exchange for financial incentives from the utility. TL allows users to shift part of their electricity consumption from high-price peak periods to low-price valley periods, thereby reducing their electricity expenses.

(1) Objective function

Electricity users adjust their consumption behavior to maximize the additional revenue obtained through participation in demand-side response programs. The objective function is formulated as

$$\max F_{\mathrm{l}} = F_{\mathrm{l,IL}} + F_{\mathrm{l,TL}} \tag{36}$$

$$F_{\mathrm{l,IL}} = \sum_{t=1}^{T} E_{l,IL}\, P^t_{\mathrm{l,IL}} \tag{37}$$

$$F_{\mathrm{l,TL}} = \sum_{t=1}^{T} E^t_{g,sel}(P^t_{\mathrm{l,IL}} + P^t_{\mathrm{l,TL}}) \tag{38}$$

where F_{l} denotes the annual additional revenue obtained by electricity users through participation in demand-side response; $F_{\mathrm{l,IL}}$ represents the subsidy income from IL; $F_{\mathrm{l,TL}}$ denotes the reduction in electricity expenses resulting from TL; $E_{\mathrm{l,IL}}$ is the unit subsidy for IL; $P^t_{\mathrm{l,IL}}$ represents the amount of load interruption in period t; $P^t_{\mathrm{l,TL}}$ denotes the quantity of load shifting in period t, where a negative value indicates load shifting into the period, and a positive value indicates load shifting out of the period.

(2) Constraints

IL constraints:

$$P^t_{\mathrm{l,IL,min}} \le P^t_{\mathrm{l,IL}} \le P^t_{\mathrm{l,IL,max}} \tag{39}$$

where $P^t_{\mathrm{l,IL,max}}$ and $P^t_{\mathrm{l,IL,min}}$ denote the upper and lower limits of the IL in period t, respectively.

TL constraints:

$$P^t_{\mathrm{l,TL,min}} \le P^t_{\mathrm{l,TL}} \le P^t_{\mathrm{l,TL,max}} \tag{40}$$

$$\sum_{t=1}^{T} P^t_{l,TL} = 0 \tag{41}$$

where $P^t_{\mathrm{l,TL,max}}$ and $P^t_{\mathrm{l,TL,min}}$ denote the upper and lower limits of the TL in period t, respectively.

4. Coordinated Planning Model and Solution Method for SGLS in DN

This study develops a coordinated planning model for SGLS in complex DN while incorporating the bounded rationality of multiple stakeholders. Electricity users determine their consumption patterns based on electricity price signals and incentive mechanisms and subsequently provide their DR information to DNOs. Meanwhile, DGOs, DNOs, and ESOs engage in an evolutionary game, each pursuing its own profit-maximization objective. By

integrating user-side DR into the decision-making process, the proposed framework yields network reinforcement plans and DG/ESS capacity allocations that reflect the bounded rationality and interactive behavior of all participating stakeholders.

4.1. Evolutionary Game Model for Multiple Stakeholders

(1) Strategy sets of game participants

In the evolutionary game, DGOs, DNOs, and ESOs are treated as three distinct populations, denoted as P_{dg}, P_{dn}, and P_{ess}, respectively. Each stakeholder constructs its strategy set based on its own decision variables, namely, DG installation capacity, network reinforcement scheme, and energy storage installation capacity.

The strategy set of DGOs is defined as $S_{\mathrm{dg}} = \{S_{\mathrm{dg1}}, S_{\mathrm{dg2}}, \ldots, S_{\mathrm{dgN}}\}$ where $S_{\mathrm{dgN}} = \{N^1_{\mathrm{dgN}}, N^2_{\mathrm{dgN}}, \cdots, N^M_{\mathrm{dgN}}\}$, and N^M_{dgN} denotes the DG installation quantity at node M under the N-th strategy. The strategy set of DNOs is given by $S_{\mathrm{dn}} = \{S_{\mathrm{dnl}}, S_{\mathrm{dn2}}, \ldots, S_{\mathrm{dnN}}\}$, $S_{\mathrm{dnN}} = \{x^{1,N}_{\mathrm{dn},1}, x^{1,N}_{\mathrm{dn},2}, \cdots, x^{1,N}_{\mathrm{dn,nl}}\}$, $x^{1,N}_{\mathrm{dn,nl}} \in [0,1]$, where $x^{1,N}_{\mathrm{dn,nl}} = 0$ indicates that line r_{nl} is not constructed under the N-th strategy, and $x^{1,N}_{\mathrm{dn,nl}} = 1$ indicates that line r_{nl} is constructed under the N-th strategy. The strategy set of ESOs is expressed as $S_{\mathrm{ess}} = \{S_{\mathrm{ess1}}, S_{\mathrm{ess2}}, \ldots, S_{\mathrm{essN}}\}$, $S_{\mathrm{essN}} = \{N^1_{\mathrm{essN}}, N^2_{\mathrm{essN}}, \cdots, N^M_{\mathrm{essN}}\}$, N^M_{essN} represents the number of storage units installed at node M under the N-th strategy.

For each population, the probability that a particular strategy is selected is defined as follows: DGO strategy selection probabilities: $p_{\mathrm{dg}} = \{p_{\mathrm{dg1}}, p_{\mathrm{dg2}}, \ldots, p_{\mathrm{dgN}}\}$, where $p_{\mathrm{dg1}} + p_{\mathrm{dg2}} + \cdots + p_{\mathrm{dgN}} = 1$; The probability that a strategy in the DNO's strategy set is selected by individuals in population P_{dn} is denoted as $p_{\mathrm{dn}} = \{p_{\mathrm{dnl}}, p_{\mathrm{dn2}}, \ldots, p_{\mathrm{dnN}}\}$, where $p_{\mathrm{dnl}} + p_{\mathrm{dn2}} + \cdots + p_{\mathrm{dnN}} = 1$. Similarly, the probability that a strategy in ESO's strategy set is selected by individuals in population P_{ess} is given by $p_{\mathrm{ess}} = \{p_{\mathrm{ess1}}, p_{\mathrm{ess2}}, \ldots, p_{\mathrm{essN}}\}$, where $p_{\mathrm{essl}} + p_{\mathrm{ess2}} + \cdots + p_{\mathrm{essN}} = 1$.

(2) Evolutionary Game Selection Mechanism

In evolutionary-game theory, stakeholders are assumed to exhibit bounded rationality, meaning that they cannot identify their optimal strategies at the outset. Instead, they iteratively adjust their strategies through learning and imitation, eventually converging to an evolutionarily stable strategy. The strategy adaptation process is governed by the replicator dynamic equations. The continuous-time replicator dynamics for the three populations are expressed as

$$\begin{cases} dp_{dgx}/dt = p_{dgx}(U_{dgx} - U_{dg}) \\ dp_{dny}/dt = p_{dny}(U_{dny} - U_{dn}) \\ dp_{essz}/dt = p_{essz}(U_{essz} - U_{ess}) \end{cases} \tag{42}$$

where p_{dgx} is the probability that an individual in population P_{dg} selects strategy S_{dgx}; U_{dgx} is the expected payoff of selecting strategy S_{dgx}; U_{dg} denotes the average expected payoff of population P_{dg}. Similarly, p_{dny} is the probability that an individual in population P_{dn} selects strategy S_{dny}; U_{dny} is the expected payoff when strategy S_{dny} is selected; U_{dn} represents the average expected payoff of population P_{dn}. Likewise, p_{essz} is the probability that an individual in population P_{ess} selects strategy S_{essz}; U_{essz} is the expected payoff associated with strategy S_{essz}; and U_{ess} denotes the average expected payoff of population P_{ess}.

Let the pure strategy sets of DGOs, DNOs, and ESOs be S_{dg} = {1,. . .,X}, S_{dn} = {1,. . .,Y}, and S_{ess} = {1,. . .,Z}, respectively. For any strategy profile (x,y,z) $\in S_{\mathrm{dg}} \times S_{\mathrm{dn}} \times S_{\mathrm{ess}}$, denote the resulting payoffs (profits) of the three stakeholders by Π_{dg}(x,y,z), Π_{dn} (x,y,z), and Π_{ess} (x,y,z), which are obtained by evaluating the corresponding profit models in Section 3 under the planning/operation outcomes associated with(x,y,z).

Given the mixed-strategy probabilities p_{dgx}, p_{dny}, and p_{essz}, the expected payoffs of choosing strategy x, y, and z are calculated as

$$U_{dgx} = \sum_{y=1}^{Y} \sum_{z=1}^{Z} p_{dny}\ p_{essz}\ \Pi_{dg}(x, y, z) \tag{43}$$

$$U_{dny} = \sum_{x=1}^{X} \sum_{z=1}^{Z} p_{dgx}\ p_{essz}\ \Pi_{dn}(x, y, z) \tag{44}$$

$$U_{essz} = \sum_{x=1}^{X} \sum_{y=1}^{Y} p_{dgx}\ p_{dny}\ \Pi_{ess}(x, y, z) \tag{45}$$

Accordingly, the average expected payoffs of the three populations are

$$U_{dg} = \sum_{x=1}^{X} p_{dgx} U_{dgx}, U_{dn} = \sum_{y=1}^{Y} p_{dny} U_{dny}, U_{ess} = \sum_{z=1}^{Z} p_{essz} U_{essz} \tag{46}$$

In numerical simulations, Equation (47) is discretized using a simulation step size as follows:

$$\begin{cases} p_{dgx}(k+1) = p_{dgx}(k) + \lambda_{dg} p_{dgx}(k)[U_{dgx}(k) - U_{dg}(k)] \\ p_{dny}(k+1) = p_{dny}(k) + \lambda_{dn} p_{dny}(k)[U_{dny}(k) - U_{dn}(k)] \\ p_{essz}(k+1) = p_{essz}(k) + \lambda_{ess} p_{essz}(k)[U_{essz}(k) - U_{ess}(k)] \end{cases} \tag{47}$$

where $p_{\mathrm{dgx}}(k)$ and $p_{\mathrm{dgx}}(k+1)$ denote the probabilities that an individual in population P_{dg} selects strategy S_{dgx} in iterations k and $k+1$, respectively; λ_{dg} is the simulation step size for population P_{dg}. Similarly, $p_{\mathrm{dny}}(k)$ and $p_{\mathrm{dny}}(k+1)$ represent the probabilities that an individual in population P_{dn} selects strategy S_{dnx} in iterations k and $k+1$, respectively; λ_{dn} is the simulation step size for population P_{dn}. Likewise, $P_{\mathrm{essz}}(k)$ and $P_{\mathrm{essz}}(k+1)$ are the probabilities that an individual in population P_{ess} selects strategy S_{sz} in iterations k and $k+1$, respectively; λ_{ess} is the simulation step size for population P_{ess}.

To enable evolutionary-game simulation with finite strategy sets, the decision variables of each stakeholder are discretized according to the physical installation granularity and the corresponding upper bounds. For DGOs, the strategy is represented by integer DG unit numbers deployed at candidate buses, subject to the maximum installation limits. For DNOs, each candidate reinforcement line is modeled as a binary decision (0: not constructed, 1: constructed). For ESOs, the storage planning strategy is defined by the integer number of storage units installed at candidate buses, bounded by the maximum allowable number. The discretization ranges are consistent with the investment and technical constraints defined in Section 3, and therefore, the strategy sets cover feasible investment decisions under the adopted planning assumptions.

4.2. Solution Method for the Coordinated SGLS Planning Model

This study develops a coordinated planning model for SGLS in DNs that accounts for the bounded rationality of multiple stakeholders. The evolutionary-game algorithm is integrated into the solution process, and the overall procedure is illustrated in Figure 2. The detailed steps for solving the planning model are as follows:

(1) Generation and screening of strategy sets: DGOs, DNOs and ESOs generate candidate strategies by enumerating discretized decision variables within their admissible ranges. To avoid including evidently infeasible candidates, strategies violating basic installation limits are removed directly. For the remaining candidates, feasibility

is further checked during payoff evaluation under the operational constraints; infeasible strategies are discarded so that they will not survive in the evolutionary process. By enumerating all discretized combinations within the prescribed ranges, the strategy space ensures coverage of potential optimal solutions under the adopted discretization granularity.

(2) Initialization of populations: The initial populations for DGOs, DNOs, and ESOs are randomly generated to serve as the starting point of the evolutionary game.

(3) Evolutionary-game process: (a) Electricity users determine their consumption behavior by synthesizing TOU pricing information and incentive mechanisms provided by the DNO. The resulting DR-adjusted load profile is then passed to the DNO; (b) individuals in each population randomly select strategies from their corresponding strategy sets until all strategies have been sampled; (c) for each combination of strategies, the profit function and payoff of each individual are computed; (d) the expected payoff of each strategy and the average expected payoff of each population are obtained; (e) based on the replicator dynamic equations, the strategy selection probabilities of each population are updated.

(4) Iteration: Steps (3) are repeated until the evolutionary process converges to an evolutionarily stable state.

(5) Output: Upon convergence, the model outputs: the DNO's network reinforcement scheme; DGO's DG capacity allocation strategy; ESO's storage capacity configuration; electricity user consumption schedules after participating in DR.

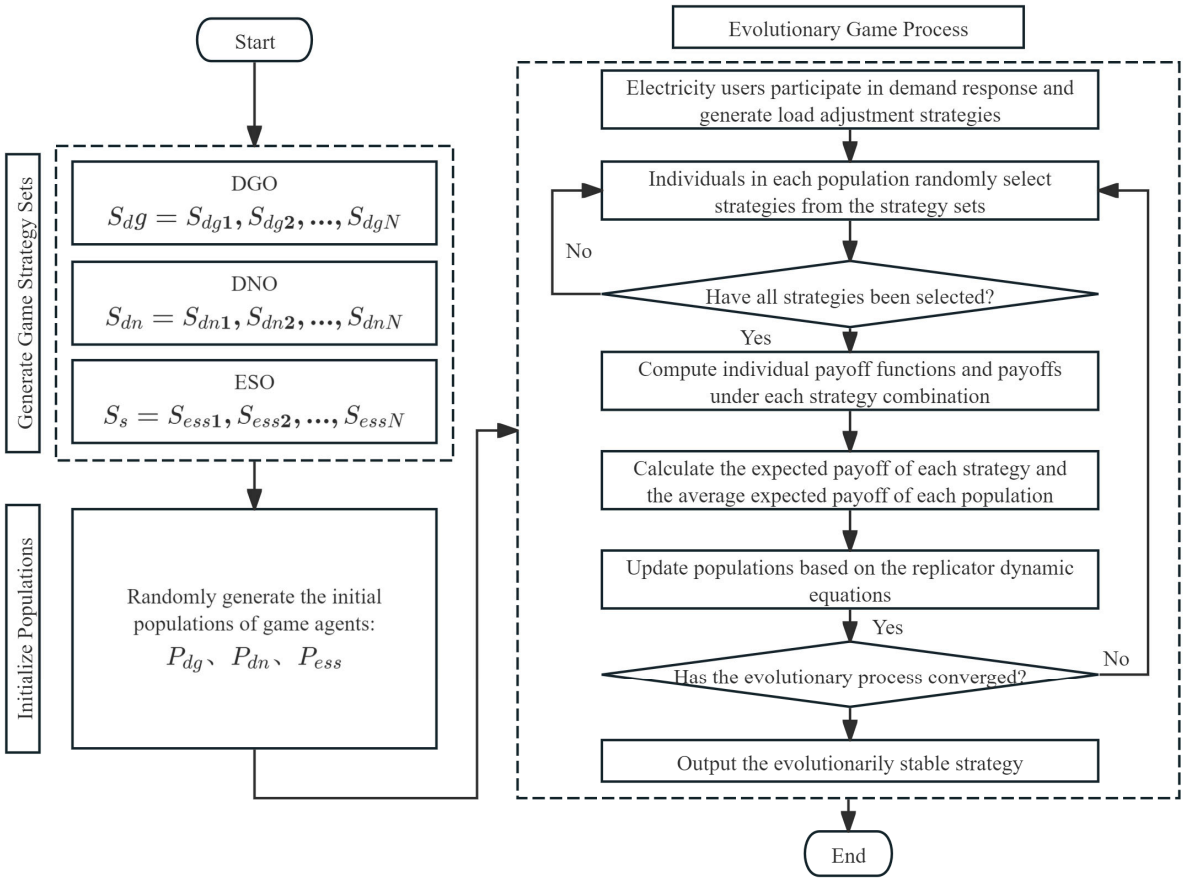


Figure 2. Flowchart of the model solution process.

5. Case Study Analysis

5.1. Key Assumptions and Baseline Settings

To validate the proposed source–network–load–storage collaborative planning model, a case study is conducted on the IEEE 33-bus distribution system. The original system capacity is 3715 kW + j2300 kvar, and its initial topology is shown in Figure 3. To accommodate the continuously growing load demand, four new load buses (Bus 34–37) are added in Table 1. After the expansion, the maximum system load increases to 4175 kW + j2560 kvar. Candidate lines for network reinforcement are marked with red dashed lines; the construction cost is CNY 100,000/km, and the line resistance and reactance are 0.27 Ω/km and 0.40 Ω/km, respectively. The corresponding line lengths and node connections are listed in Table 1. The purchasing price of electricity from the upper-level grid is set to CNY 0.4/kWh. The planning horizon is 10 years, and the annual discount rate is 6%. The discount rate mainly affects the planning outcomes through the capital recovery factor (CRF), which annualizes the upfront investments of DG, network reinforcement, and ESSs into comparable annual costs, and therefore, influences the payoff evaluation of long-term strategies.

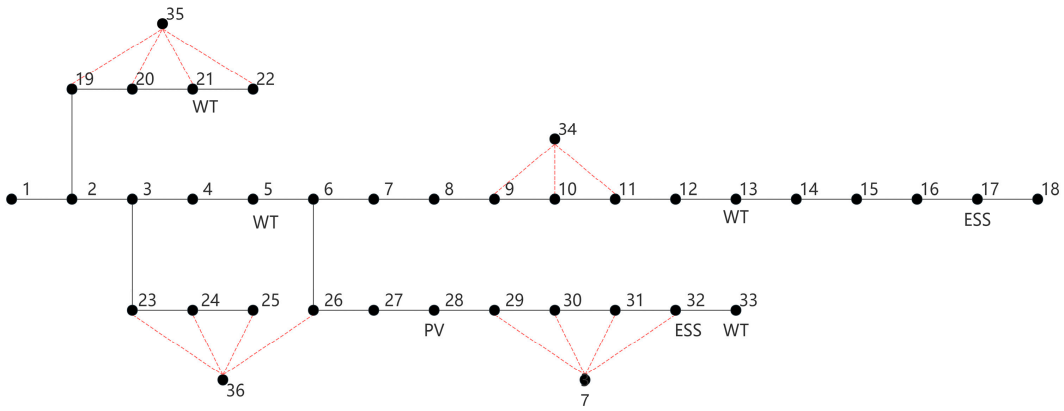


Figure 3. Topology of the DN.

Table 1. Locations and lengths of newly added nodes.

To Bus	From Bus	Line Length (km)
34	9	3.34
	10	3.08
	11	2.47
35	19	2.46
	20	2.08
	21	3.69
	22	3.39
36	23	2.72
	24	2.1
	25	2.28
	26	1.91
37	29	3.52
	30	2.06
	31	2.13
	32	2.48

On the demand side, all loads are assumed to be TLs participating in price-based DR. The TOU tariff structure is provided in Table 2. The parameters of DG and ESSs used in this case study are summarized in Table 3. The peak–valley price spread determines the strength of the price signal, directly shaping both (i) the arbitrage potential of ESSs (charging at low-price hours and discharging at high-price hours) and (ii) the incentive for demand shifting in the DR module; hence, it is a key driver of benefit allocation among DNOs/ESOs (and the overall coordination effect). Bus 25 is designated as an IL node, with the interruptible period defined as 11:00–22:00 and an IL compensation rate of CNY 0.4/kWh.

Table 2. TOU electricity price parameters.

Time Period	Electricity Price (CNY·kWh^{-1})
Peak 8:00–10:00, 16:00–21:00	0.575
Shoulder 5:00–8:00, 10:00–11:00, 14:00–16:00, 21:00–23:00	0.425
Valley 00:00–5:00, 11:00–14:00, 23:00–24:00	0.325

Table 3. Parameters of wind power, photovoltaic generation, and energy storage systems.

Type	Parameter	Value
wind	Maximum installation capacity (kW)	600
	Investment cost (CNY·kWh^{-1})	4000
	O&M cost (CNY·kWh^{-1})	0.15
	Electricity selling price (CNY·kWh^{-1})	0.2
	Candidate installation buses	5, 13, 21, 33
PV	Maximum installation capacity (kW)	600
	Investment cost (CNY·kWh^{-1})	4000
	O&M cost (CNY·kWh^{-1})	0.15
	Electricity selling price (CNY·kWh^{-1})	0.34
	Candidate installation bus	28
ESS	Maximum installation capacity	240 kW/800 kWh
	Investment cost (CNY·kWh^{-1})	600
	O&M cost (CNY·kWh^{-1})	0.01
	Upper/lower SOC limits	0.9/0.1
	Charging/discharging efficiency	0.9
	Candidate installation buses	17, 32

The initial time-series data for load and renewable generation are obtained from the operation records of a real distribution network in Northeast China. Specifically, a full-year dataset (January–December, 365 days) is collected, including hourly active-power demand at the feeder/substation level and the aggregated hourly active-power outputs of grid-connected wind and photovoltaic units in the same area (Δt = 1 h). Prior to scenario extraction, the raw data are time-aligned and cleaned by filling occasional missing samples via linear interpolation and filtering abnormal spikes using a standard z-score rule. Finally, the load, wind, and PV series are normalized by their annual maxima to form per-unit profiles for subsequent clustering and planning analysis.

Based on the preprocessed one-year dataset, each day is represented by concatenating the 24 h per-unit profiles of load, wind power, and photovoltaic generation. A Gaussian mixture model (GMM) is employed to cluster these daily vectors into four representative typical-day scenarios. The cluster centroids and their occurrence probabilities are used to construct the typical-day profiles shown in Figure 4, which are then used for subsequent planning and simulation analysis. In practical operation, such typical-day profiles can also be constructed from short-term forecasts; for example, machine-learning PV forecasting models can provide day-ahead inputs to support operational optimization in decentralized systems [26].

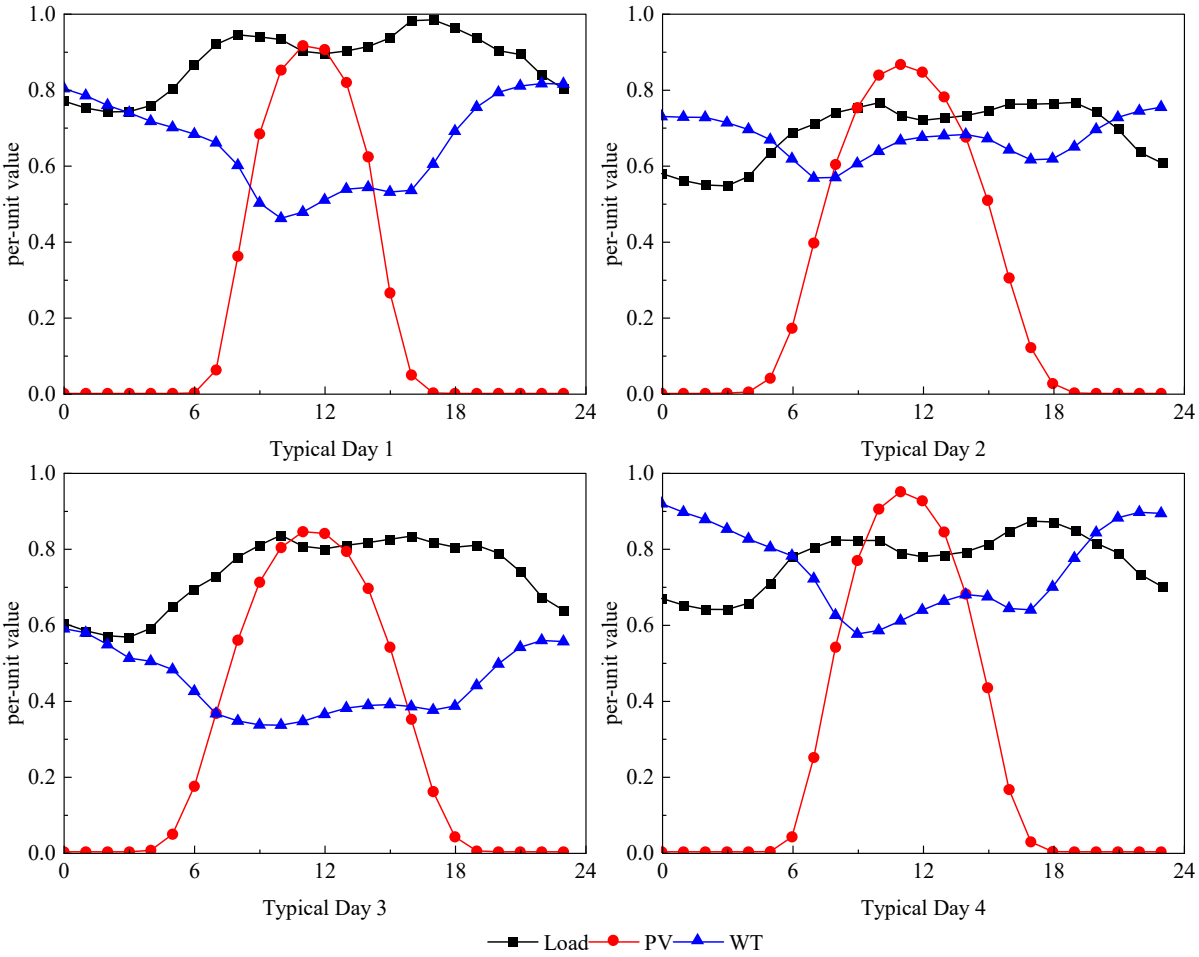


Figure 4. Typical-day profiles of load, wind power, and photovoltaic generation.

All numerical experiments are implemented in MATLAB 2025b. The demand-response scheduling of electricity users is formulated as a linear programming problem and solved using the Optimization Toolbox solver linprog. The evolutionary-game simulation is performed by a discrete-time replicator-dynamics iteration with Monte Carlo sampling until convergence. Typical-day clustering is conducted via a GMM using the Statistics and Machine Learning Toolbox (https://ww2.mathworks.cn/products/statistics.html?s_tid=AO_PR_info, accessed on 15 December 2025).

5.2. Results Analysis

Under consideration of user-side DR, the proposed collaborative planning model incorporates the bounded rationality of stakeholders and determines the optimal planning scheme for DN reinforcement, DG deployment, and ESS allocation through an evolutionary game among DGOs, DNOs, and ESOs.

The evolutionary stable strategies emerging from the game, along with the corresponding variations in strategy selection probabilities during the evolution process, are illustrated in Figure 5.

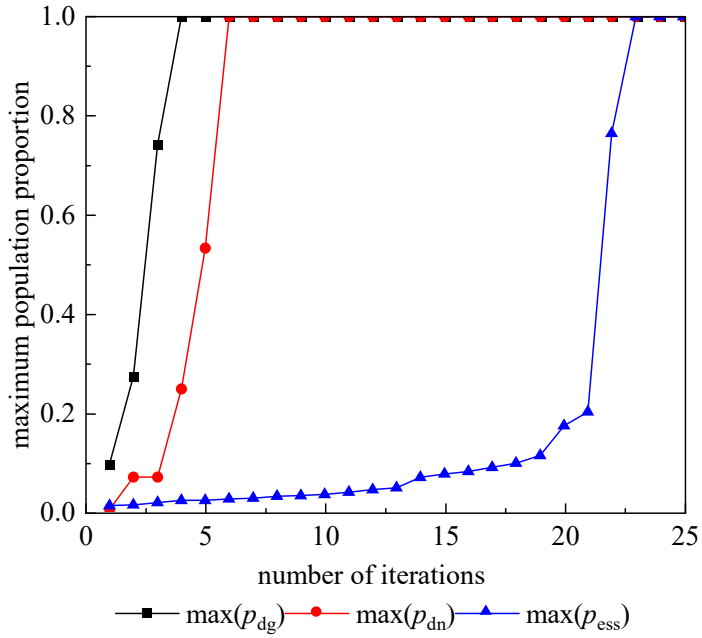


Figure 5. Convergence curves of the evolutionary game.

During the evolutionary process, the strategy selection probabilities of DGOs, DNOs, and ESOs are continuously updated with each iteration. Ultimately, the probability of selecting a single strategy converges to 1, while the probabilities associated with all other strategies converge to 0. This indicates that, as the iterations progress, individuals within each population gradually refine their strategic choices through continuous learning and imitation, eventually reaching an evolutionarily stable state. The evolutionary-game approach effectively captures the bounded rationality of real-world decision-makers and highlights the iterative process through which agents converge by repeatedly learning, imitating, and adjusting strategies.

(1) Allocation and Profit Analysis of Source–Grid–Storage Planning

To further assess how different typical-day scenarios influence the benefit structure of the coordinated SGLS planning model, Table 4 presents the optimal installation capacities of DG and energy storage under four representative typical days. The ten-year total revenues and corresponding net present values (NPV) for DGOs, DNOs, and ESOs are summarized in Table 5. The results indicate that the load profiles and renewable output patterns associated with different typical days significantly affect both the overall system economics and the benefit distribution among stakeholders.

As shown in Table 4, the optimal DG and ESS installation schemes across the four typical days exhibit both consistency and scenario-specific diversity.

First, in Typical Day 1 and Typical Day 3, the model selects the same configuration—1900 kW of wind, 0 kW of PV capacity, and 1600 kWh of storage. This reflects that, under the load–resource conditions represented by these two typical days, wind power provides higher utilization potential than PV. PV generation is not selected because the early-morning and evening load levels are relatively high or the midday load is insufficient to absorb PV output, leading to limited economic benefits. This indicates that the load curves and renewable-resource characteristics of Typical Days 1 and 3 are more compatible with wind power as the primary renewable resource.

Table 4. Installed capacities of distributed generation and energy storage under typical-day scenarios.

Typical Day	Indicator	Installed Capacity
1	wind	1900 kW
	PV	0
	ESS	1600 kWh
2	wind	2150 kW
	PV	250 kW
	ESS	1600 kWh
3	wind	1900 kW
	PV	0
	ESS	1600 kWh
4	wind	2150 kW
	PV	250 kW
	ESS	1600 kWh

Table 5. Revenues of different stakeholders under typical-day scenarios.

Typical Day	Stakeholder	Ten-Year Total Revenue (10^4 CNY)	Ten-Year Net Revenue (10^4 CNY)
1	DGO	615	453
	DNO	2234	1644
	ESO	26	19
2	DGO	653	481
	DNO	2441	1796
	ESO	26	19
3	DGO	69	51
	DNO	1628	1198
	ESO	26	19
4	DGO	870	640
	DNO	2697	1985
	ESO	26	19

Second, in Typical Days 2 and 4, the model deploys a portfolio of 2150 kW of wind, 250 kW of PV capacity, and 1600 kWh of storage. Unlike Typical Days 1 and 3, the appearance of non-zero PV installation in Typical Days 2 and 4 implies that the midday load is higher or the matching between PV output and demand is stronger, allowing PV to provide effective energy substitution during peak periods and thereby improve system economics. The increase in wind capacity from 1900 kW to 2150 kW further suggests that, under these scenarios, the marginal benefit of wind generation increases due to more favorable resource conditions, enabling wind and PV to operate synergistically.

It is noteworthy that the optimal storage capacity remains constant at 1600 kWh across all typical-day scenarios. This indicates that, within this planning context, storage primarily functions to perform peak shaving and valley filling, increase renewable energy accommodation, and reduce power purchase costs. The variations in load shapes across

typical days are insufficient to motivate the model to expand storage capacity. Thus, storage sizing is influenced more by price signals and the overall system economic structure than by the characteristics of individual typical days.

These findings demonstrate that typical-day clustering effectively captures the structural differences in annual load patterns and renewable output characteristics. The resulting optimal configurations exhibit clear structural regularities: when PV is poorly aligned with the load profile, the model tends to favor larger wind installations; conversely, when midday loads are higher or wind-PV complementarities are stronger, a combined wind-PV configuration emerges. This validates the capability of the typical-day-based optimization framework to autonomously select economically optimal SGLS configurations under diverse resource and load scenarios.

Analysis of the data in Table 5 reveals that typical-day variations exert a significant influence on the ten-year total and net revenues of DGOs, the DNO, and ESOs. However, the sensitivity of each stakeholder to these variations differs markedly.

From the perspective of DGOs, revenue exhibits a clear upward trend as the typical-day index increases. The ten-year total revenue rises from CNY 6.15 million in Typical Day 1 to CNY 8.70 million in Typical Day 4, while the corresponding net revenue increases from CNY 4.53 million to CNY 6.42 million. This indicates that typical days characterized by more favorable renewable output conditions significantly enhance DG substitution capability and profitability. The highest DG revenue occurs under Typical Day 4, suggesting that this daily load profile and renewable availability pattern provides the most advantageous conditions for DG utilization.

Note that the unusually low DGO revenue on Typical Day 3 is caused by the renewable-resource condition represented by this typical-day scenario. As shown in Figure 4, Typical Day 3 corresponds to a low renewable-output (particularly low wind) profile. Since the planning configuration under Typical Day 3 installs wind at only 1900 kW with 0 PV, the DGO's revenue is almost entirely determined by wind electricity sales. Consequently, the limited wind availability, together with the relatively lower load level indicated by the reduced DNO revenue in Table 5, results in a much smaller amount of renewable energy being utilized and sold, leading to the sharp decline in DGO revenue, CNY 69×10^4.

DNOs consistently achieves the highest revenue among the three stakeholders. Its ten-year total revenue increases from CNY 22.34 million (Typical Day 1) to CNY 26.97 million (Typical Day 4), while net revenue increases from CNY 16.44 million to CNY 19.85 million. The monotonic increase reflects that Typical Day 4 is associated with the highest overall load level and the largest electricity purchase volume, enabling the grid to earn more through retail electricity sales. In contrast, Typical Day 3 results in significantly lower total revenue (CNY 16.28 million) and net revenue (CNY 11.98 million), highlighting the adverse impact of lower load levels on grid-side economic returns.

In comparison, the revenues of the ESS remain highly stable across all four typical days. The ten-year total revenue remains approximately CNY 260,000, with net present values around CNY 190,000, indicating minimal sensitivity to typical-day variation. This stability suggests that, under the current TOU price structure and modest peak–valley price differentials, the profitability of small-scale ESS installations is driven primarily by fixed arbitrage opportunities rather than renewable variability. Moreover, ESS profitability is considerably lower than that of DG and DN, highlighting that the existing market mechanism does not fully compensate for the flexibility value provided by storage in peak shaving, load shifting, and renewable accommodation. To stimulate investment in independent storage, additional incentive mechanisms—such as capacity payments, ancillary-service compensation, or increased peak–valley price spreads—may be needed.

From a market-design perspective, the above mechanisms can be viewed as monetizing different components of the flexibility value provided by ESS. A capacity remuneration scheme can compensate storage for firm capacity and peak support that are not fully reflected by energy arbitrage under a modest peak–valley spread. Ancillary-service markets (e.g., regulation and reserves) provide an additional revenue stream that rewards fast response and ramping capability. Moreover, enlarging the peak–valley spread or adopting more granular time-varying pricing can strengthen the arbitrage signal, thereby improving ESO investment incentives. These measures are complementary and could be implemented through performance-based payments or long-term contracts.

The economic comparison across the four typical days demonstrates that load shapes and renewable generation patterns directly determine the benefit distribution within the SGLS system. Higher peak loads and larger peak–valley price spreads significantly increase DG and DNO revenues. When renewable energy generation aligns more closely with high-price periods, DG profitability improves further due to reduced curtailment and enhanced substitution of grid electricity. Composite wind-PV configurations outperform single-resource configurations in most scenarios, reflecting their superior adaptability to diverse load conditions. Meanwhile, ESS revenue remains stable but relatively low, suggesting that its flexibility value is not fully monetized under current electricity pricing mechanisms.

Overall, the classification and weighting of typical days exert a substantial impact on the economic evaluation of the system. They shape renewable energy utilization, influence the effectiveness of price signals, and determine the revenue distribution among stakeholders. Thus, typical-day selection is a critical component of comprehensive energy system planning.

The behavioral characteristics of the four typical-day scenarios significantly affect the economic performance of the coordinated SGLS planning schemes. Compared with single-source renewable configurations, wind-PV hybrid deployments yield superior economic outcomes, particularly under Typical Day 4, where all stakeholders achieve their highest ten-year revenues. Furthermore, under the existing pricing mechanism, DNOs remain the primary beneficiary, whereas ESO gains limited economic return—underscoring the necessity of refining compensation mechanisms to enhance the attractiveness of ESS investment.

(2) Necessity of Considering Multi-Agent Game Mechanisms

To evaluate the necessity of incorporating a multi-agent evolutionary game into the planning framework, we compare the complex DN planning outcomes and stakeholder revenue distributions with and without the game-theoretic mechanism. The resulting planning decisions are presented in Table 6, while the revenues of different stakeholders are summarized in Table 7.

Table 6. Distribution network planning results.

	Indicator	**Installed Capacity**
With game-theoretic interaction	wind	1900 kw
	PV	0
	ESS	1600 kwh
Without game-theoretic interaction	wind	1900 kw
	PV	0
	ESS	0

Table 7. Revenues of different stakeholders.

Typical Day	Stakeholder	Ten-Year Total Revenue (10^4 CNY)	Ten-Year Net Revenue (10^4 CNY)
With game-theoretic interaction	DG	615	453
	Grid	2234	1644
	ESS	26	19
Without game-theoretic interaction	DG	615	453
	Grid	2308	1699
	ESS	0	0

As shown in Table 6, the incorporation of a multi-agent game mechanism has a substantial impact on both the planning outcomes and the distribution of benefits among stakeholders. When the game-theoretic interaction is considered, the system deploys 1900 kW of WT, 0 kW of PV, and 1600 kWh of energy storage. This allocation enables ESOs to earn stable profits through price arbitrage. In contrast, when the game mechanism is not considered, the storage investment is completely eliminated by the planning model. This indicates that conventional single-objective planning tends to prioritize the interests of DNOs and fails to reflect the investment incentives of ESOs.

In terms of revenues, Table 7 shows that DG earnings remain unchanged between the two scenarios. DNO's revenue increases slightly in the non-game scenario due to higher electricity purchases; however, ESO's revenue drops to zero, resulting in weakened coordination among stakeholders. By comparison, the game-theoretic approach not only enables reasonable storage deployment but also yields a system-wide revenue structure that more closely matches the interactions observed in real electricity markets. These results confirm the necessity and rationality of introducing evolutionary-game mechanisms into SGLS coordinated planning.

(3) Impact of DR on benefit allocation and coordination

To evaluate how DR affects multi-stakeholder coordination, we compare two scenarios—with DR and without DR—across four typical-day cases (Tables 5 and 8), focusing on the 10-year total and net revenues of the DNO, DGO, and ESO.

DNO: In all typical days, the DNO's revenues decrease after DR is introduced. For Typical Day 1, the 10-year total revenue drops from CNY 25.02 to 22.34 million, and the net revenue decreases from CNY 18.41 to 16.44 million. This indicates that DR suppresses peak demand via load-side regulation, reducing the DNO's margin associated with high-price periods and high-load operation, and confirming a clear peak-shaving effect.

DGO: The DGO's revenues remain unchanged under both scenarios for all typical days (e.g., CNY 6.15 million total and CNY 4.53 million net in Typical Day 1). This suggests that, under the current case settings, DR does not directly affect DG output or revenue; system improvements are achieved through load adjustment rather than reducing renewable returns.

ESO: In contrast, the ESO benefits from DR in all typical days. For Typical Day 1, the ESO's 10-year total revenue increases from CNY 0.21 to 0.26 million, and the net revenue rises from CNY 0.15 to 0.19 million. DR improves the operating environment and provides more stable opportunities for storage, enhancing its economic performance.

Overall, DR reshapes the benefit-allocation structure while keeping DGO revenues stable, indicating a shift in regulation responsibility from the grid side toward the load-and-storage side and clarifying functional coordination among SGLS entities.

Table 8. The revenues of each stakeholder without considering DR.

Typical Day	Stakeholder	Ten-Year Total Revenue (104 CNY)	Ten-Year Net Revenue (104 CNY)
1	DG	615	453
	Grid	2502	1841
	ESS	21	15
2	DG	653	481
	Grid	2650	1951
	ESS	21	15
3	DG	69	51
	Grid	1856	1366
	ESS	21	15
4	DG	870	640
	Grid	2926	2154
	ESS	21	15

6. Conclusions

This study develops a multi-agent evolutionary-game-based coordinated planning model for active DNs under high renewable energy penetration. By integrating DGOs, DNOs, ESOs, and user-side DR, the proposed framework captures the strategy learning and dynamic adjustment processes of stakeholders under bounded rationality. It enables coordinated optimization of SGLS resources with respect to economic efficiency, operational security, and system flexibility. The case studies demonstrate the following key findings:

(1) The evolutionary game mechanism effectively drives the strategies of the three operators toward an evolutionarily stable equilibrium, thereby avoiding the suboptimal configurations that commonly arise in conventional planning due to conflicting stakeholder objectives.

(2) Distinct installation patterns emerge across typical-day scenarios. On days where the load profile aligns poorly with PV output, the system favors wind-dominated configurations. Conversely, when solar irradiance is strong and midday demand is high, a complementary wind-PV deployment becomes the optimal choice.

(3) Benefit analysis reveals substantial heterogeneity among stakeholders. DNOs remain the primary beneficiary, while DG profits increase with improved renewable generation conditions. ESS revenues, however, remain relatively stable but modest, indicating that the current market mechanisms still fall short of fully reflecting the system-level flexibility value provided by storage.

Overall, the proposed evolutionary-game-based coordinated planning framework provides an effective theoretical foundation and methodological reference for promoting multi-agent collaboration and maximizing renewable energy utilization in active DNs.

Author Contributions: Conceptualization, Y.S., X.L., X.W. and L.J.; methodology, R.Z. and D.W.; software, X.W. and L.J.; formal analysis, X.G.; investigation, Y.Y.; resources, X.L.; data curation, J.W. and X.X.; writing—original draft preparation, Y.L.; writing—review and editing, Z.O. and Z.M. All authors have read and agreed to the published version of the manuscript.

Funding: This research was funded by the Research on Business Models of Source–Grid–Load–Storage Coordinated Demand Response under the Revitalization of Northeast China's Old Industrial Base, 2025 (SGJLJY00LNJS2500036).

Data Availability Statement: Data available on request due to restrictions privacy. The data presented in this study are available on request from the corresponding author because the modeled data for this study was obtained from the corresponding author, and the raw data required permission from the first author.

Conflicts of Interest: Authors Yu Shi, Yiwen Yao, Jing Wang, Xiaomin Lu, Xinhong Wang, Dingheng Wang, Xuefeng Gao and Xin Xu were employed by the Power Economic Research Institute of Jilin Electric Power Co., Ltd. Author Rui Zhou was employed by State Grid Jilin Electric Power Co., Ltd. The remaining authors declare that the research was conducted in the absence of any commercial or financial relationships that could be construed as a potential conflict of interest. This study was supported and sponsored by Power Economic Research Institute of Jilin Electric Power Co., Ltd. and State Grid Jilin Electric Power Co., Ltd. State Key Laboratory of Coastal and Offshore Engineering, Dalian University of Technology completed the study and informed Power Economic Research Institute of Jilin Electric Power Co., Ltd. and State Grid Jilin Electric Power Co., Ltd. of the results, which were published with Power Economic Research Institute of Jilin Electric Power Co., Ltd. and State Grid Jilin Electric Power Co., Ltd.'s permission. There are no other conflicts of interest.

References

1. Adewuyi, O.B.; Aki, H. Optimal planning for high renewable energy integration considering demand response, uncertainties, and operational performance flexibility. *Energy* **2024**, *313*, 134021. [CrossRef]
2. Dini, A.; Hassankashi, A.; Pirouzi, S.; Lehtonen, M.; Arandian, B.; Baziar, A.A. A flexible-reliable operation optimization model of the networked energy hubs with distributed generations, energy storage systems and demand response. *Energy* **2022**, *239*, 121923. [CrossRef]
3. Wang, C.; Liu, C.; Chen, J.; Zhang, G. Cooperative planning of renewable energy generation and multi-timescale flexible resources in active distribution networks. *Appl. Energy* **2024**, *356*, 122429. [CrossRef]
4. Li, A.; Xiao, F.; Zhang, C.; Fan, C. Attention-based interpretable neural network for building cooling load prediction. *Appl. Energy* **2021**, *299*, 117238. [CrossRef]
5. Zhang, J.; Wang, C.; Zuo, J.; Gao, C.; Zheng, S.; Cheng, R.; Duan, Y.; Wang, Y. Multi-Stage Rolling Grid Expansion Planning for Distribution Networks Considering Conditional Value at Risk. *Energies* **2024**, *17*, 5134. [CrossRef]
6. Cai, D.; Wang, Z.; Miao, S.; Chen, R.; Zheng, Z.; Zhou, K. Wind-Photovoltaic-Energy Storage System Collaborative Planning Strategy Considering the Morphological Evolution of the Transmission and Distribution Network. *Energies* **2022**, *15*, 1481. [CrossRef]
7. Gao, H.; Li, Y.; He, S.; Tang, Z.; Liu, J. Distributionally robust planning for power distribution network considering multi-energy station enabled integrated demand response. *Energy* **2024**, *306*, 132460. [CrossRef]
8. He, Y.; Wu, H.; Bi, R.; Qiu, R.; Ding, M.; Sun, M.; Xu, B.; Sun, L. Coordinated planning of distributed generation and soft open points in active distribution network based on complete information dynamic game. *Int. J. Electr. Power Energy Syst.* **2022**, *138*, 107953. [CrossRef]
9. Song, X.; Shu, M.; Wei, Y.; Liu, J. A Study on the Multi-Agent Based Comprehensive Benefits Simulation Analysis and Synergistic Optimization Strategy of Distributed Energy in China. *Energies* **2018**, *11*, 3260. [CrossRef]
10. Dong, X.; Quan, C.; Jiang, T. Optimal Planning of Integrated Energy Systems Based on Coupled CCHP. *Energies* **2018**, *11*, 2621. [CrossRef]
11. Li, J.; Wang, T.; Tang, S.; Jiang, J.; Chen, S. Planning distribution network using the multi-agent game and distribution system operators. *Front. Energy Res.* **2023**, *11*, 1244394. [CrossRef]
12. Wang, C.; Liu, C.; Zhou, X.; Zhang, G. Flexibility-based expansion planning of active distribution networks considering optimal operation of multi-community integrated energy systems. *Energy* **2024**, *307*, 132601. [CrossRef]
13. Zhou, M.; Ma, F.; Jin, W. Long-term cost planning of data-driven wind-storage hybrid systems. *Renew. Energy* **2024**, *223*, 120073. [CrossRef]
14. Mao, Y.; Yuan, J.; Jiao, X. Optimal Operation of Combined Cooling, Heating, and Power Systems with High-Penetration Renewables: A State-of-the-Art Review. *Processes* **2025**, *13*, 2595. [CrossRef]
15. Liu, Y.; Yang, N.; Dong, B.; Wu, L.; Yan, J.; Shen, X.; Xing, C.; Liu, S.; Huang, Y. Multi-Lateral Participants Decision-Making: A Distribution System Planning Approach with Incomplete Information Game. *IEEE Access* **2020**, *8*, 88933–88950. [CrossRef]

16. Saldaña-González, A.E.; Aragüés-Peñalba, M.; Sumper, A. Distribution network planning method: Integration of a recurrent neural network model for the prediction of scenarios. *Electr. Power Syst. Res.* **2024**, *229*, 110125. [CrossRef]
17. Mehrjerdi, H. Simultaneous load leveling and voltage profile improvement in distribution networks by optimal battery storage planning. *Energy* **2019**, *181*, 916–926. [CrossRef]
18. Suryakiran, B.V.; Nizami, S.; Verma, A.; Saha, T.K.; Mishra, S. A DSO-based day-ahead market mechanism for optimal operational planning of active distribution network. *Energy* **2023**, *282*, 128902. [CrossRef]
19. Mao, Y.; Cai, Z.; Jiao, X.; Long, D. Multi-timescale optimization scheduling of integrated energy systems oriented towards generalized energy storage services. *Sci. Rep.* **2025**, *15*, 8549. [CrossRef]
20. Budi, R.F.S.; Sarjiya; Hadi, S.P. Multi-level game theory model for partially deregulated generation expansion planning. *Energy* **2021**, *237*, 121565. [CrossRef]
21. Yang, N.; Xiong, Z.; Ding, L.; Liu, Y.; Wu, L.; Liu, Z.; Shen, X.; Zhu, B.; Li, Z.; Huang, Y. A game-based power system planning approach considering real options and coordination of all types of participants. *Energy* **2024**, *312*, 133400. [CrossRef]
22. Zhou, J.; Chen, K.; Wang, W. A Power Evolution Game Model and Its Application Contained in Virtual Power Plants. *Energies* **2023**, *16*, 4373. [CrossRef]
23. Wu, Z.; Xu, Z.; Gu, W.; Zhou, S.; Yang, X. Decentralized Game-Based Robustly Planning Scheme for Distribution Network and Microgrids Considering Bilateral Energy Trading. *IEEE Trans. Sustain. Energy* **2022**, *13*, 803–817. [CrossRef]
24. Singh, A.; Sethi, B.K.; Kumar, A.; Singh, D.; Misra, R.K. Three-Level Hierarchical Management of Active Distribution System with Multimicrogrid. *IEEE Syst. J.* **2023**, *17*, 605–616. [CrossRef]
25. Li, J.; Zhou, B.; Yao, W.; Zhao, W.; Cheng, R.; Ou, M.; Wang, T.; Mao, T. Research on dynamic robust planning method for active distribution network considering correlation. *Front. Energy Res.* **2023**, *11*, 1338136. [CrossRef]
26. Alhassan, M.O.; Gyamfi, S.; Aboagye, B.; Diawuo, F.A.; Kwarteng, M. In-situ PV generation forecasting of utility-scale solar power plants in Ghana: Single and hybrid machine learning approaches. *Sol. Energy Adv.* **2025**, *5*, 100124. [CrossRef]

Disclaimer/Publisher's Note: The statements, opinions and data contained in all publications are solely those of the individual author(s) and contributor(s) and not of MDPI and/or the editor(s). MDPI and/or the editor(s) disclaim responsibility for any injury to people or property resulting from any ideas, methods, instructions or products referred to in the content.